IMPACT OF PROCESSING ON STRUCTURE AND PROPERTIES OF CARBON FIBER AND EFFECTS ON COMPOSITE PERFORMANCE

Benjamin Vaughan, Harini Dasarathy, Xinzhang Zhou, Jennifer McInnis, Peter Ferrin
Hexcel Corporation
281 Tresser Blvd, 16th Floor
Stamford CT 3261

ABSTRACT

Carbon fibers derived from PAN precursors are finding ever expanded adoption into industrial applications such as transportation and energy as well as the typical aerospace composite venues. We describe the development of carbon structure as a function of conversion from polymeric precursor. The description of periodic structures using scattering techniques such as XRD are interpreted in light of other data derived from techniques such as spectroscopy, porosimetry, and traditional chemical methods. The talk will aim to explain how certain properties important to composite performance are affected by process and the limiting structures that are formed. Additionally, comments and data associated with testing of carbon fibers and derived specimen will be presented.

1. INTRODUCTION

1.1 Carbon Fiber Process and Properties

As the carbon fiber industry developed, a common set of unit operations evolved into what we know today as the carbon fiber process; namely, oxidation, low temperature carbonization (aka tar removal), high temperature treatment (possibly HM furnace), surface treatment and sizing. Several types of precursor can be converted into carbon fiber with this basic process, but we will focus on polyacrylonitrile (PAN) precursors and their resulting structure and properties. Each of these operations is independently important and the morphology of the fiber leaving one process will affect how it changes in the subsequent unit operation.

Some of the earliest descriptions of the connections between process and carbon fiber structure can be found in the literature related to Shindo's work at the Industrial Research Institute and the parallel efforts of Johnson and Watt at the Royal Aircraft Establishment (***1***,***2***,***3***) Shindo was able to establish the basics of what we know today about the structure and properties of carbon fiber from X-ray diffraction (XRD) data.

The literature also tells us that small adjustments to an existing conversion process can make a tremendous difference in carbon fiber properties. We keep this in mind today as we make changes to our process. Perhaps the first carbon fiber process improvement can be credited to Johnson and Watt who realized that the Young's modulus of carbon fiber could be improved by resisting the shrinkage of the precursor during the oxidation or stabilization step. (***2***) Just introducing this concept, that holding tension, relaxing tension or stretching the fiber could alter its properties was a major step forward in the processing of PAN-based carbon fiber. Although

at the time tension may have appeared to be a minor player, the carbon fiber properties we enjoy today would not be possible without out the manipulation of this simple process parameter. (***4***) We acknowledge that composite properties are heavily dependent on the interaction between the carbon fiber and the matrix; however this presentation will focus on fiber and associated structural features primarily.

2. EXPERIMENTATION

2.1 Methods & Instrumentation

Raman Spectra were collected with a Thermo Scientific DXR Raman Microscope. Raman spectra were collected in a DXR Raman microscope equipped with a 532nm laser. The spot size was ~0.8μm. Data for one sample consists of five spectra collected in five different spots and then averaged to give one composite spectra for analysis.

Data for *X-ray Diffraction* was collected on a Rigaku 3kW SmartLab X-Ray Diffractometer with a Cu source. All scans were collected in transmission mode at either a phi of 0° (fiber parallel with the floor) or a phi of 90° (fiber perpendicular to the floor). The crystal sizes were determined using the Scherrer Equation with a shape factor of 0.89. The fiber orientation was taken from FWHM of the 2θ peak at 25.6° after a phi rotation. Unless stated otherwise, samples were run in transmission with parallel beam optics and a scintillation detector.

Fibers for Scanning Electron Microscope (*SEM) analysis* were etched in an electrochemical bath containing 0.1N NaOH and observed on a model Hatachi S-4000 Field Emission SEM.

Porosimeter analysis for surface area, pore volume and pore size was carried out using a Quantachrome Autosorb iQ. The probe gas used was nitrogen at 77K. Several different glass and quartz cells sizes were used based on the required size of the sample. The nitrogen adsorption isotherms were used for pore size analysis using a quench solid density functional theory (QSDFT) model for nitrogen on carbon which assumes slit shapes for the micropores and cylinders for the mesopores.

Inverse Gas Chromatography (IGC) analysis of the carbon fiber surface was made using a Surface Measurement Systems Surface Energy Analyzer. Alkanes including hexane, heptane, octane and nonane were used to determine dispersive surface energies by a polarization approach (***5***), with Gutmann K_a value (***5***) determined using the following set of acidic and basic probes: methylene chloride, ethyl acetate, n-propanol, ethanol, acetone, and acetonitrile. All measurements are done at 50 °C with entropic contributions considered negligible. Probe molecules are introduced at nominal surface coverages between 0.1 and 0.01 monolayer. High purity helium (99.999%, US Welding) was used as the carrier gas. Methane was injected both before and after probes to calculate the dead volume.

Cyclic Voltammetry measurements for specific conductivity measurements were made in a solution of 0.1 M KCl or ammonium bicarbonate in distilled water using a conventional three-electron cell, with the carbon fiber was used as the working electrode, with a Pt wire counter electrode and a Ag/AgCl reference electrode. Voltage was varied from 0 – 0.15 V versus the Ag/AgCl reference at a rate of 10 mV/sec using a Model 600C Series Potentiostat (CH Instruments), with five successive sweeps, with the capacitance calculated as the average capacitance of the last four sweeps. All measurements were completed at room temperature.

3. RESULTS

In the following sections we will discuss characterization at each process step. The methods employed will include Raman spectroscopy, XRD, electrochemical etching with SEM, IGC, cyclic voltammetry and porosimetery. In a few sections we will discuss some of the implications of using these measurements to drive process and what effect this could have on composite properties and performance.

3.1 Oxidation

Oxidation is the first step the precursor fiber will encounter in the conversion process. There are certainly differences between the way manufacturers control tension during this processing step due to the different methods manufacturers use to spin their precursor. One must manage the built-in orientation of the precursor to influence the orientation in the oxidized "ox" fiber which will eventually be fed into the next unit operation, the low temperature furnace. The tension will partly control the amount of order or disorder in the resulting ox fiber. The other factor is the temperature profile in oxidation as the precursor is allowed to react to desired density (usually 1.32-1.44 g/cc) and filament diameter. The temperature profile will also define the speed at which one is able to process the precursor as the primary limitations are control of the cyclization/oxidation reactions and one's ability to remove heat and gaseous species from the system.

There are a host of common chemical and physical methods one can use to monitor the oxidation process including Infrared Spectroscopy (IR), Differential Scanning Calorimetry (DSC), O_2 content, fiber density, water uptake, and chemical shrinkage. (***4***) Even though every carbon fiber manufacturer utilizes this process, there is still significant debate with respect to how exactly the chemical and structural changes are taking place. To broach this question, we utilize Raman spectroscopy to interrogate the changes occurring during oxidation.

3.1.1 Raman Spectroscopy

The use of Raman spectroscopy as a tool in characterization of PAN and carbon fiber surfaces has become more refined in recent years so that more than crystal sizes can be determined. In the first stage of stabilization through oxidation, the initial highly-crystalline structure of PAN fiber is lost and the carbon atoms gradually rearrange into cyclized structures.

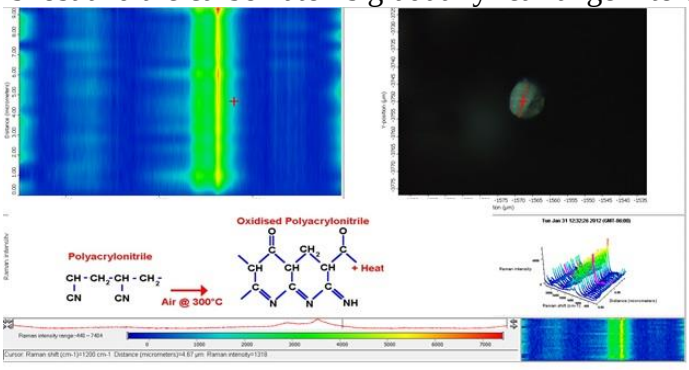

Figure 1: Map across filament cross-section

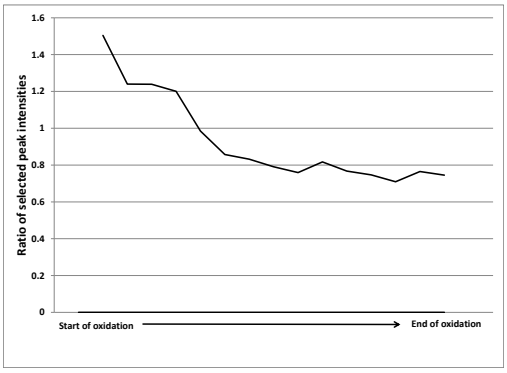

Figure 2: Reaction progress from peak ratio

Uniformity of oxidation across the filament depends on both processing parameters and filament diameter. This depth- dependent behavior can be traced by collecting the spectra across the

filament cross-section at regular predetermined intervals and compiling them together as a map file (Figure 1). The map is then split into different individual spectra for further data analysis. Ratios of selected peaks indicate the reaction progress with time and temperature (Figure 2).

An example of the typical spectra collected across the face of an oxidized PAN fiber can be seen below. The larger diameter filaments show a skin/core effect with higher level of oxidation in the skin and lower level in the center part of the filament (Figure 3). By contrast, smaller diameter fibers show uniform oxidation levels across the filaments (Figure 4). The ratio of ordered/cyclized carbon peaks ($1580cm^{-1}$ / ~$1355cm^{-1}$) corresponds to degree of oxidation at each point. This correlation helps us to select processing conditions which we can use to tune the reaction rate and therefore the final structure obtained.

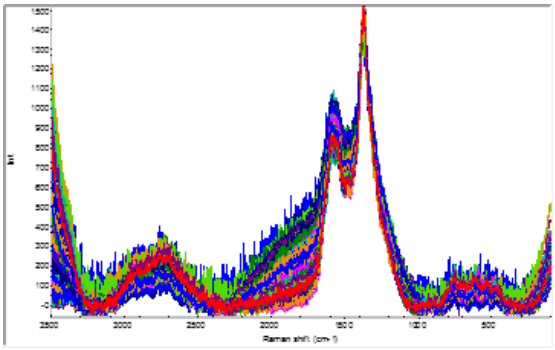

Figure 3: Spectra of large diameter filament

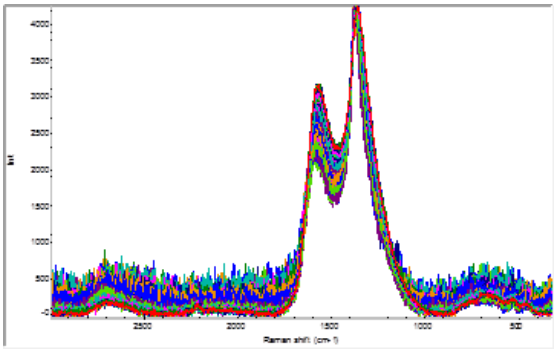

Figure 4: Spectra of small diameter filament

3.2 High Temperature Furnace (HT)

The next processing steps include tar removal and high temperature treatment of the fiber. Each manufacturer maintains proprietary furnace profiles for these steps and we know from experience that these profiles can have a major effect on the resulting carbon fiber and composite properties. We will focus on the HT fiber measurements and properties and assume the Low Temperature Furnace (LT) is a constant for the purposes of this paper. We will discuss the use of XRD, Raman and SEM as it pertains to carbon fiber structure in this section.

3.2.1 X-Ray Diffraction

PAN-based carbon fiber contains crystals with a structure similar to that of graphite. However, these structures are best described as turbostratic carbon as they do not achieve the same degree of ordering as observed in graphite. The sp^2 hybridized carbon atoms are arranged in a honeycomb lattice that is aligned parallel to the length of the fiber. Analysis of the fiber or powder by XRD allows us to characterize the crystal size present in the carbon fiber and the degree of orientation of these crystallites can also be determined.

We have been using this technique to profile our furnace in terms of crystal growth, to better understand the morphological changes through carbonization. What we have found is that the crystals do not grow at a constant rate during processing. This fact was accurately measured by cutting a length of fiber from inside the furnace. The fiber was then cut into equal sections and each section was analyzed by XRD. Looking at the ratio of crystal growth in each section to the total crystal growth in the furnace (Figure 5), it is apparent that there is a stepwise nature to the crystal growth which could indicate the carbon is undergoing different phase transitions as it passes through. In addition, the analysis shows that the L_a and L_c crystal dimensions grow at

approximately the same rate. This tells us that there is little change in the overall crystal shape as the fiber passes through the furnace.

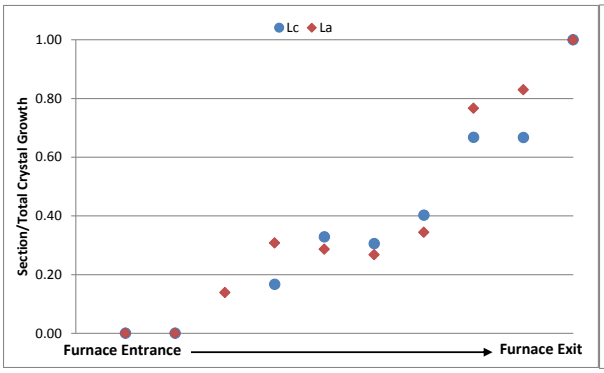

Figure 5: Crystal growth in carbon fiber inside the HT

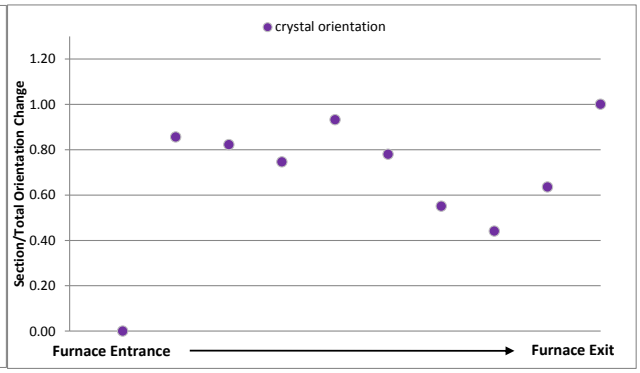

Figure 6: Increased orientation of crystals in HT

We can also monitor the orientation of the above mentioned crystals as a function of position in the high temperature furnace. Overall, the crystals inside of the carbon fiber become more orientated as the fiber traverses the furnace (**Error! Reference source not found.**). This increased orientation occurs almost immediately after the fiber enters the entrance of the high temperature furnace, with the final fiber orientation approximately equal to the orientation reached early in the furnace. There appears to be a temporary drop in the orientation in ¾ of the way through the furnace which indicates again that a phase transition and rearrangement is likely occurring at these temperatures. There are theories in the literature which describe the coalescence of crystals through the amorphous phase but we are not convinced this is the only mode of crystal growth in carbon fiber. (***1***) The drop in orientation opens up the possibility that there is enough mobility present for the structure to actually rearrange at these high temperatures.

We have used this technique to monitor crystal size as a guide to tailor our process for certain parameters requested by customers. Controlling this crystal growth via temperature has allowed us to not only improve the properties of the carbon fiber but has also helped us to improve certain composite properties. This will be covered more specifically in another section of the paper.

3.2.2 Raman Spectroscopy

We have outlined the use of Raman to follow the structural changes present in the oxidation step of carbon fiber processing. Similarly, analyses of fibers from the post stabilization process of carbonization provide structural information and allow optimization of conversion processes to achieve desired CF properties. Typical spectra shown of PAN-based carbon fiber with various moduli were obtained by processing at temperatures from~1200 to 2500 °C and are shown in Figure 7. Structural changes by selective etching of carbon fiber (see SEM analysis) also can be traced by subtle change in the peak heights of ordered carbon (~1585 cm^{-1}) and disordered peaks (~1360 cm^{-1}) (Figure 8). The disordered peak decreased with the etching processes.

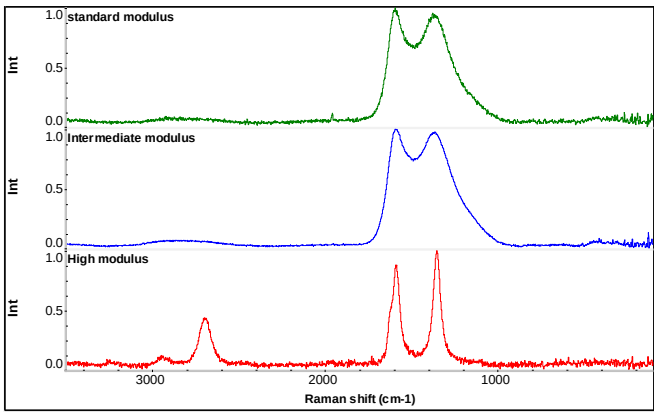

Figure 7: Typical Raman spectra of PAN-based CFs

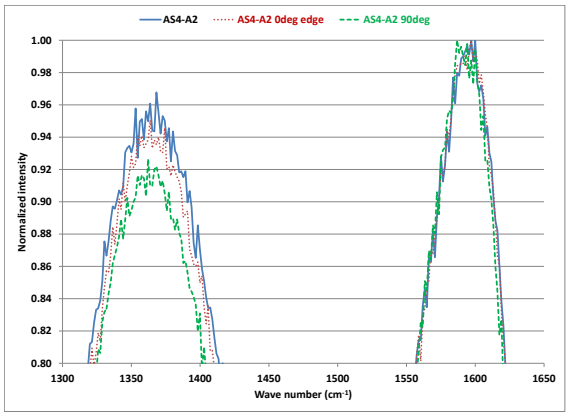

Figure 8: Raman spectra of etched fibers

Another area in where Raman spectroscopy data has been useful is to correlate the progress of the structural changes in carbonization to tailor desired CF properties. This is a complementary analysis to the XRD data described in the section above. As in the XRD analysis, the sections represent a particular temperature/time and stretch history that the fiber has experienced (Figure 9). Raman analysis can be directly related to the modulus of the carbon fiber. Therefore, Raman spectral intensities at certain identified wavelengths provide information of the modulus buildup rate and allow us to select process parameters to obtain a desired modulus. A comparison of the intensities at a certain wavelength from the measured Raman spectra (fiber surface structure) along with orientation angle determined by XRD analyses (structure in the bulk of the fiber) show us that both decrease as the fiber passes from one end of the HT furnace to the other indicating (Figure 10) structural changes on the surface and bulk are occurring simultaneously.

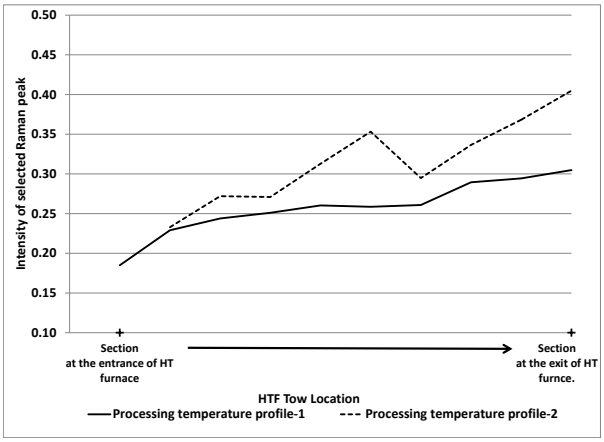

Figure 9: Raman intensity from HT sections

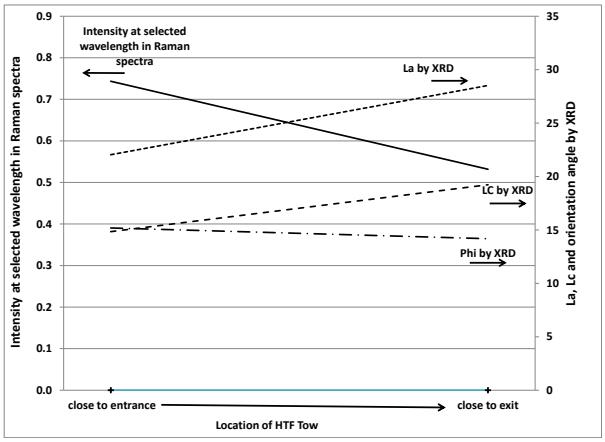

Figure 10: Data from Raman and XRD

3.2.3 Etching and SEM

Another tool we have been using to evaluate the structure of fiber processed through the HT is etching in combination with SEM analysis. There are several different types of etching techniques one could imagine using in this circumstance but we have opted for electrochemical etching due to the inherent conductivity of the fiber. The etching mechanism of carbon fiber in a basic environment is shown in Figure 11. The hydroxyl anion promotes an oxygen-generating reaction and because the carbon fiber acts as the anode, the oxidation process occurs everywhere on the carbon fiber surface. Using this process, even over a long period of time (30 minutes),

results in a smooth surface for the filaments as illustrated in **Error! Reference source not found.**. The three fibers in the foreground are etched while the three filaments in the background are as supplied.

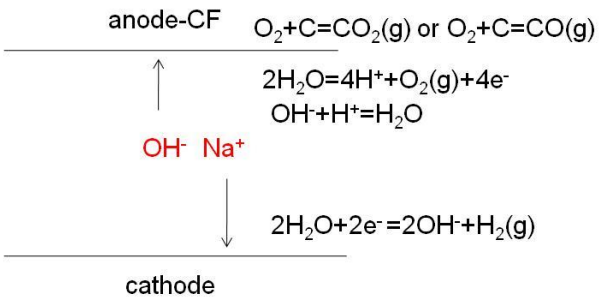

Figure 11: Etching process for CF: NaOH as the electrolyte

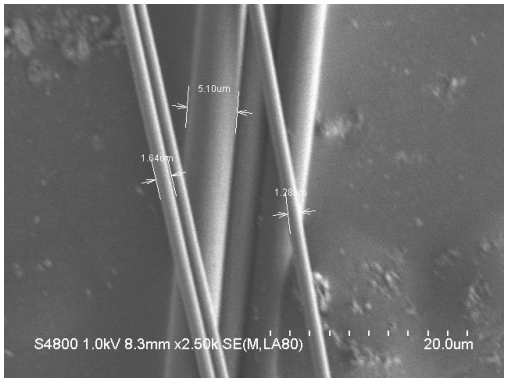

Figure 12: (Foreground) Etched Filaments

An improvement on the above technique has allowed us to obtain the microstructures of carbon fiber at the sub-filament level. At a low current condition and a high sodium hydroxide concentration, "skeletal structures" appear and can be observed with SEM after etching polished panel specimens. As shown in Figure 13-14, uniform skeletal structures can be seen after this etching technique has been applied to some of our IM fibers. We believe that during this process, the amorphous phases in the carbon fiber are being etching away while the crystalline graphite portions are maintained. The sizes of the graphite grains and the holes for these IM fibers are about the same; both are in the range of 10-50 nm.

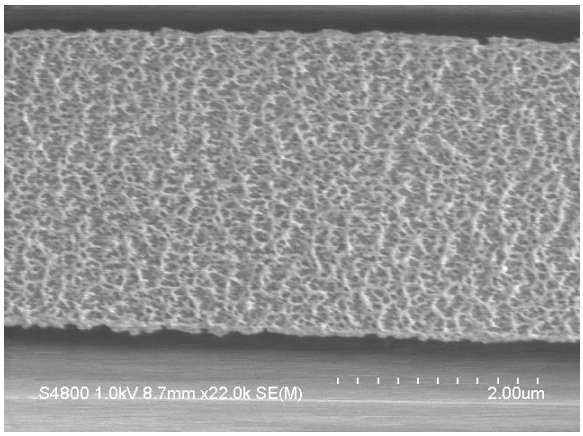

Figure 13: Skeletal structures in IM7

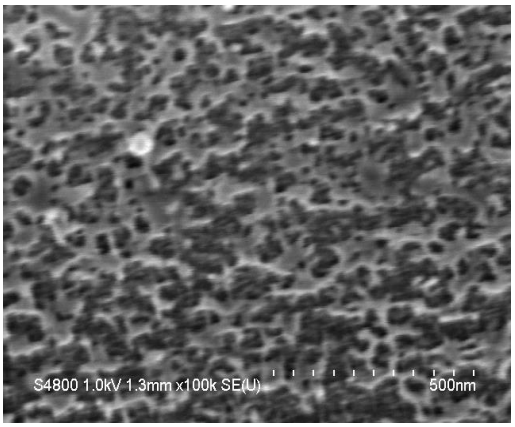

Figure 14: IM7 at higher magnification

We have also used this technique to probe the skin-core structures in some of our fibers. While no clear skin-core structure is observed using this technique when we look at our HM or IM7 fibers, under a similar etching environment, AS4 has shown obvious signs of skin-core structures as illustrated in Figure 15. What we have found is that the skin and core are separated by a transitional band rather than an abrupt line. It can be seen in Figure 16-18 that the morphologies on either side of the band have similar microstructures although at a different density. It appears from the SEM that the crystals in the band region are more interconnected compared to the skin

and core regions. The reason for this is not fully understood at this point and needs further investigation.

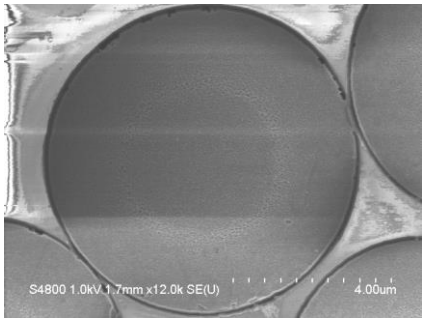

Figure 15: AS4 skin-core structure as observed from etching and SEM analysis

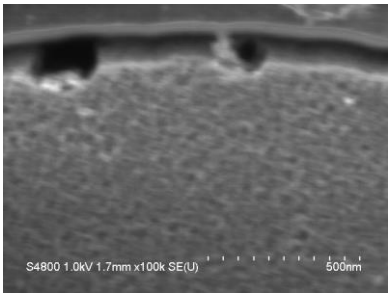

Figure 16: "skin" from Figure 12

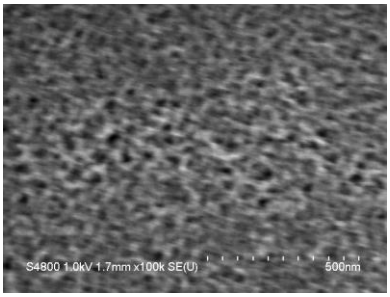

Figure 17: "band" from Figure 12

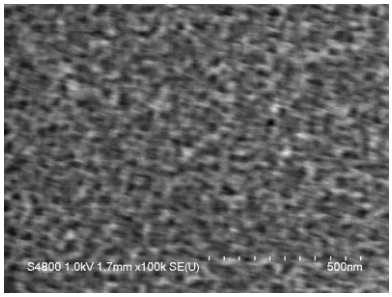

Figure 18: "core" from Figure 12

Figure 19 shows a comparison between the microstructures of Hexcel AS4, IM7 and HM fibers treated with the described electrochemical etching technique at three different magnifications. The top row of micrographs shows the entire etched filaments in the field of view. As the reader can see a clear skin-core structure exists in the AS4 fiber while the IM7 and HM fibers show no transition in their morphologies across the width if the filament. This leads us to believe that the crystallinity of the HM and IM fibers should be consistent from edge to core while a gradient of crystallinity would exist for the AS4 fibers. This is obviously due to the thickness of the fibers being processed and the conditions under which they are processed not only through the HT but also in oxidation.

As one zooms closer to take a look at these microstructures (2^{nd} and 3^{rd} row of Figure 19) it is reasonable to say that the general form of the microstructures observed in AS4 are similar to those observed in the IM7 and HM samples. They can be described as interconnected crystalline phases separated by a more amorphous phase which was removed during etching. However, the sizes of these crystalline phases are not as we would have predicted based on the processing conditions used to make them (2^{nd} row Figure 19). The order of the observed crystallite regions is as follows; AS4 > IM7 > HM. We know from XRD that the crystal size grows with increasing heat treatment. The size of the crystalline phases should be in the following order HM > IM7 > AS4. The microstructures developed during these processes are certainly related in some way to the structures observed in the micrographs but may be more complex than we originally thought. We plan to perform more SEM work specifically aimed at HM fibers made from AS4, and IM7 at temperatures from 1800 °C to 2500 °C to sort out the development of these structures as temperature increases.

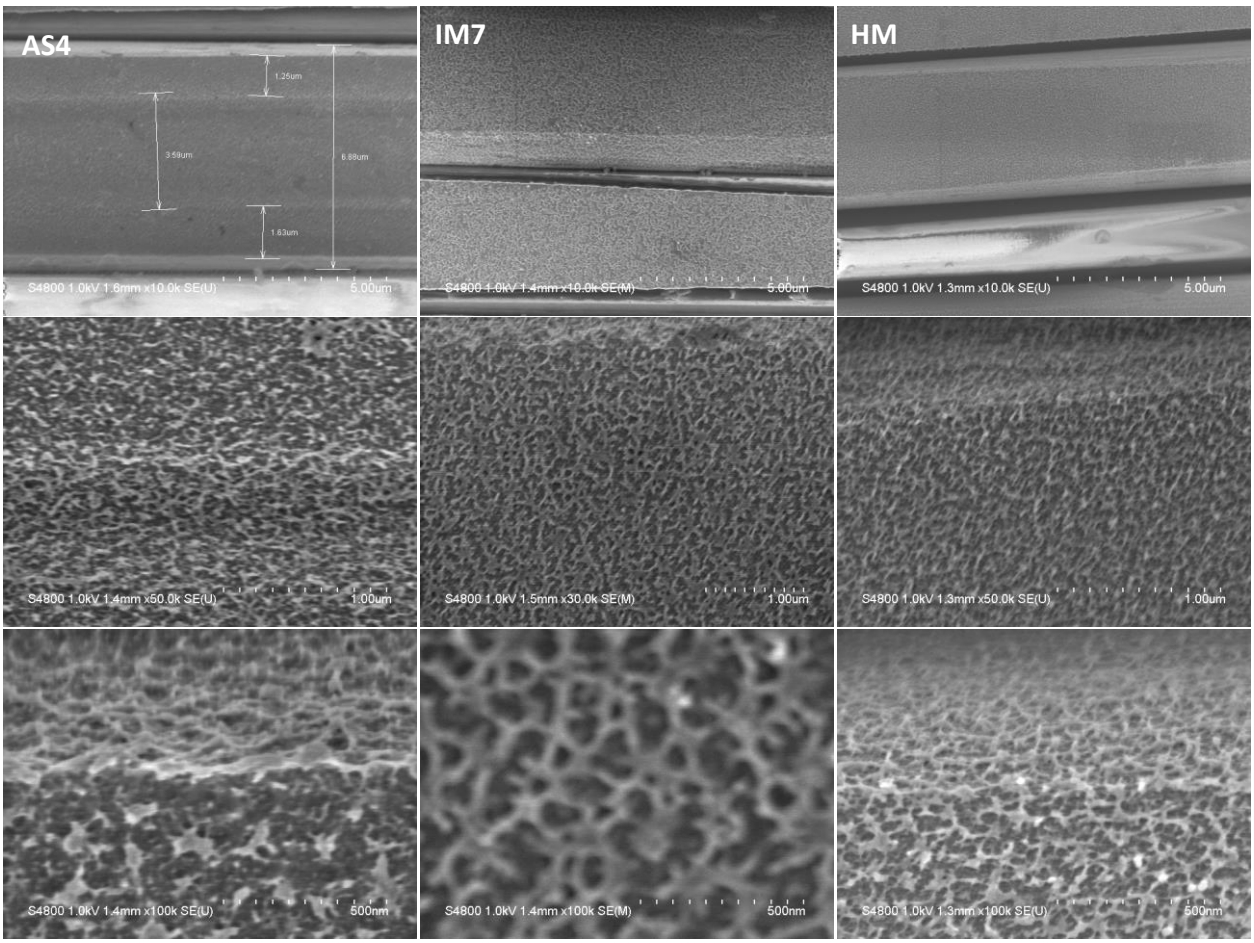

Figure 19: Structural comparisons among AS4, IM7 and HM carbon fibers

One piece of evidence supporting the theory that these are crystalline phases is observed with Raman spectroscopy. The spectra show that a lower ID/IG ratio exists for the microstructures in in the above mentioned standard modulus fiber. Raman spectra of the edge of the fiber cross section shows greater crystallinity compared to the center of the fiber. Also when the fiber is turned on its side and scanned the crystallinity is even higher as the structures on the outside of these fibers are the most highly etched and therefore highly crystalline.

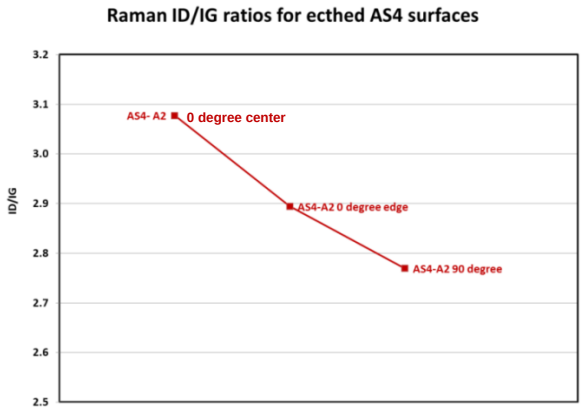

Figure 20: Raman ID/IG ratios for etched microstructures

3.2.4 Porosimetery

Microvoids oriented along the fiber axis are known to exist in carbon fiber and have been reported on in detail. (***6***) In most cases the studies have involved small angle x-ray scattering (SAXS) as the method used to measure these pores but we have been using a different technique, gas adsorption, to probe the differences in our typical products. The samples for this analysis were prepared by freeze-milling in order to expose as much of the internal pore structure as possible. We will refer to the measured pore volume as accessible pore volume because we know if the internal network is not connected, and the particle sizes are not small enough, we will not reach all of the void volume with this method. Also this method is only applicable in the micro and meso pore range (<35nm pore width) therefore, any pores larger than ~ 40nm will not be captured with this method.

As we look at the outside of carbon fiber with this technique we measure very low pore volumes and we believe that more than 98% of the available micro and meso porosity is inside the fiber. We have compared pore sizes measured on the outside of the fiber to those measured on the inside and believe many of the same pore sizes are present in both regions. It is valuable from a structural understanding level to know what pore sizes and volumes are present inside our carbon fiber but we also believe this gives some insight into the pores likely on the surface that are difficult to measure due to the low number present. We will present data based on nitrogen isotherms collected at 77K with very long equilibrium times to give us the best possible resolution.

Below in Figure 21 we show the pore size distribution (PSD) for a series of our products in the micro and meso porous regions. The products compared are a typical standard modulus (SM), intermediate modulus (IM) and high modulus carbon fiber (HM). Recall, these are pores present on the inside of the fiber. We can see that the SM and IM fibers have almost identical pore widths while the HM fiber appears to have additional pore sizes present due to the higher temperatures it has been treated with. This indicates some type of rearrangement or relaxation has taken place in the HM furnace which allows for these additional pores to be present in significant enough quantities that they can be measured. The typical micorpores present in the SM and IM fibers are at 0.65nm and 1.01nm while the HM fiber splits this region into three pore sides at 0.67, 0.84, and 1.28nm. These micropores make up approximately 20% of the available total (micro, meso) pore volume present in the samples.

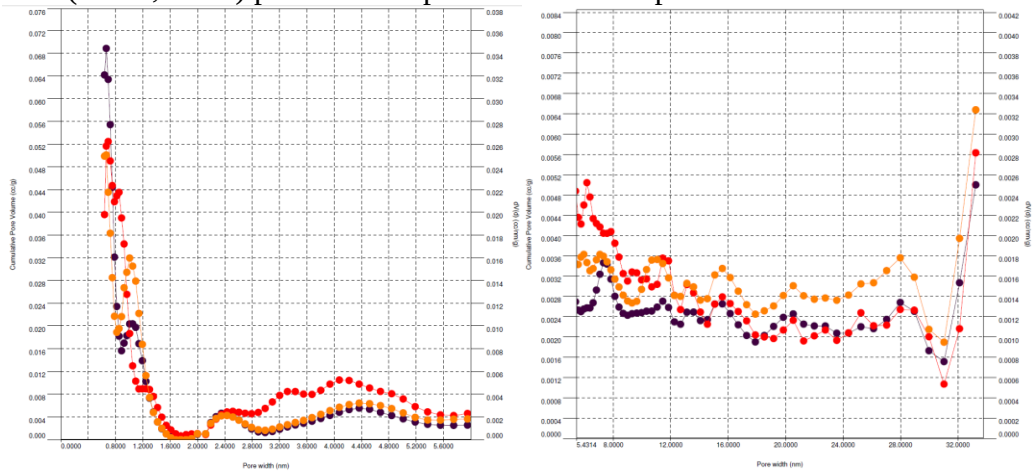

Figure 21: PSD for red = HM, black = SM, orange =IM carbon fiber. Left side micropore region and right side meso-pore region

The mesopore region includes pore sizes above 2nm and this region contains most of the measureable available pore volume. The more defined region includes IM and SM pores at 2.44nm and 4.4nm. The HM fiber as mentioned above has a more developed pore structure and well defined pores can be seen at 2.44, 3.35, and 4.15 nm. The rest of the mesopore region is much noisier and I have amplified it (Figure 21 right side) so the reader can see there are some pore sizes but it is more difficult to call these defined pores because of the low resolution. This region represents 2/3 of the available pore volume and may be more like ends of connected channels as observed and reported above in the etching section. The well-defined pore regions are likely related to the more highly ordered part of the CF (1/3) while the less defined regions likely go with the less ordered regions one might find in CF.

3.3 Surface Treatment

The last carbon fiber process step we will discuss in this paper is surface treatment. Several different methods of surface treatment of CF have been employed over the years including gas oxidation with various gas mixtures (including steam), liquid phase oxidation and the more commonly employed anodic oxidation. Anodic oxidation takes advantage of the inherent conductivity of carbon fiber in conjunction with an electrolyte bath. The cathode is submerged in the bath at some distance from the carbon fiber which acts as the anode (conductive SS roller is positioned above the bath to complete the circuit). The setup produces oxygen at the CF anode and hydrogen at the cathode. The hope is that the surface is then chemically modified to include chemical groups like =C=O, -COOH, -COOX, -CO3 and possibly even some amine chemistries based on the electrolyte used in the bath.

3.3.1 Inverse Gas Chromatography

The strength and toughness of the fiber-resin interface is an important characteristic that affects composite bulk properties, such as shear strength. (***4***,***7***) One way to control this is by oxidizing the carbon fiber surface using one of several methods described in the academic or patent literature, notably plasma treatment, electrochemical oxidation, or wet chemical oxidation. Carbon fiber treated in this way shows improved adhesion to resin systems. Unfortunately, over-oxidation of the carbon fiber can lead to degradation in other properties due to fiber damage.

Quantifying the extent of oxidation of the carbon fiber becomes tremendously important so as to maximize adhesion without compromising fiber integrity. Several surface science methods can be employed for this purpose, including spectroscopic methods (e.g., X-ray photoelectron Spectroscopy (XPS)), microscopy, contact angle analysis, and others. (***7***) One that has shown some benefit not only in quantifying the extent and type of oxidation, but also exploring the morphology on the surface is IGC.

Those interested in a detailed explanation of the theory behind IGC are referred to excellent reviews elsewhere. (***5***) (***8***) In short, however, a series of well-defined probes of varying dispersive energies, acidities, and basicities are injected in a gas chromatograph and passed over a packed column of the solid phase of interest. The retention time of these probes through the column governed by a combination of factors, including probe characteristics, IGC setup, amount of probe injected, and the affinity of the probe to the fiber surface. By carefully controlling other factors, a significant amount of information can be derived about the surface in question, particularly the surface energy, entropy, acidity/basicity of the surface and the

accessible surface area. Using a set of probes with varying affinities and also varying the amount injected, one can explore the heterogeneity of the surface. (***9***) IGC has been used for carbon fiber characterization in the past (***7***), although generally in the 'infinite-dilution' regime where only the strongest-affinity sites of the fiber are sampled by the probe molecules. More recently, finite-dilution methods have been developed, where the probe is introduced at specific submonolayer coverages. This allows for a better understanding of whether an oxidation method is changing a large fraction of the sites or just a few selected sites on the surface.

In one illustration of the power of this technique, we took a typical intermediate-modulus fiber and varied the intensity of its surface oxidation, and then measured the K_a, a measure of the acid interaction of the fiber with Gutmann bases (***5***) at a series of probe coverages. The result (Figure 22) is that at the lowest coverages tested, we observed lower acidities for a fiber subjected to milder oxidation conditions, specifically at the lowest probe coverages. This is in agreement with other studies using different methods such as XPS and titration to measure acidity. (***7***) However, at higher coverages (even 5% of a monolayer), the differences between fibers are much less pronounced. This significant heterogeneity in the fiber response to oxidation suggests that there exists a population of more easily-modified sites while the majority of the carbon fiber sites are not available for these types of oxidation. These easily modified sites are a small fraction of the overall surface for example edge or defect sites. Moreover, there appears to be a step change in oxidation behavior; while a slightly more aggressive oxidation did not affect the higher-coverage sites, eventually those sites are affected (as shown by the difference in oxidation two and three in Figure 22). This type of behavior may be important in establishing control parameters for surface treatment, especially if there is a correlation between such threshold levels and laminate properties.

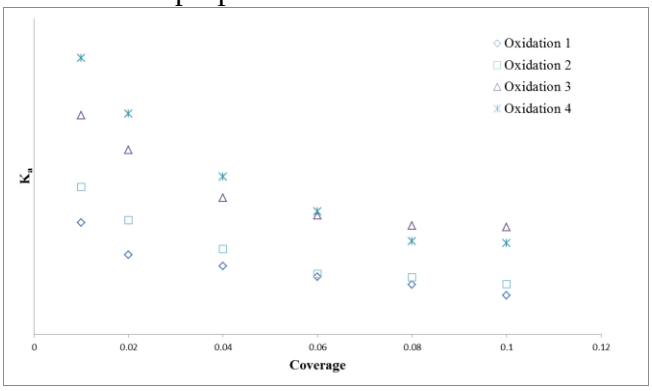

Figure 22: Acidity (as measured by Ka) as a function of coverage for a set of oxidation conditions. Oxidation 1 - most mild conditions, Oxidation 4 - most severe oxidation conditions. Coverage is in units of monolayer of probe.

The measured IGC surface characteristics of these fibers, such as the K_a (acidity parameter) described in **Error! Reference source not found.**, do appear to play a role in governing macroscopic laminate behavior. Figure 23 shows one such correlation. In this case, we prepared a series of intermediate modulus fibers subjected to different surface treatment intensities. We then measured the K_a at a fixed coverage and compared it to open hole tensile strength in laminates made with these fibers. As one can see, there is a good correlation between the measured acidity of the fiber via IGC and this important laminate parameter. The laminate with the higher acidity fiber clearly shows a decrease in open-hole tensile strength.

This suggests that by carefully controlling the surface treatment one can engineer the desired macro-scale laminate properties. Such correlations are strongest at certain probe coverages, which may indicate that only some fraction of the fiber is actually playing a role in the adhesion between fiber and resin and thus affecting the toughness of the overall composite. As demonstrated here, by measuring and controlling the surface properties of the fiber, one can have an effect on the overall fiber as well as laminate properties.

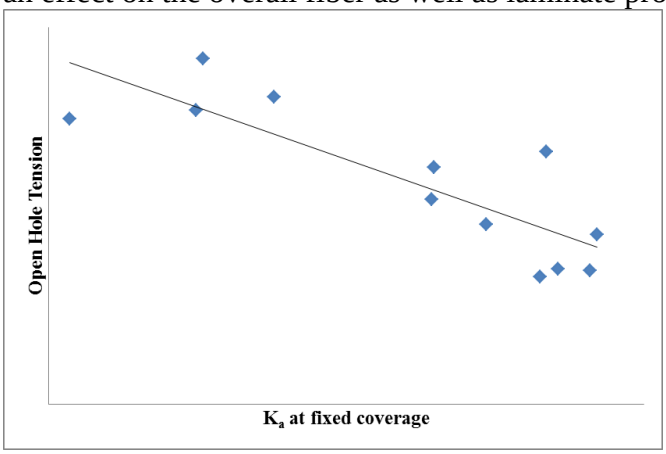

Figure 23: Measured open-hole tension strengths of a number of intermediate modulus fibers as a function of their acidity at a fixed coverage.

3.3.2 Cyclic Voltammetry

In addition to probing the surface chemistry of carbon fiber using IGC, we have been exploring other methods. A technique that appears to complement the IGC measurements we have been making on surface treated carbon fiber is cyclic voltammetry. We are still in the process of developing this method for our application but it is showing promise. Our aim is to quantify the amount of oxygen on the surface of treated carbon fiber. In a composite, the strength of the interfacial bonds is related to the amount of oxygen on the fiber surface, as the oxygen allows for electron transfer between the resin and fiber at the interface. (***10***) (***7***)

In addition to its potential role in bond creation at the interface, the oxygen on the surface will change the electrochemical properties of a carbon fiber. (***11***) (***12***) An increase in certain types of oxygen groups in activated carbon was correlated with the specific capacitance of the activated carbon, potentially quinones. (***11***) We measure the capacitance of the fiber by performing cyclic voltammetry in a typical electrolyte (e.g., 0.1 M KCl or ammonium bicarbonate) at low voltages and a fixed sweep rate. At these voltages (0 – 0.15 vs. Ag/AgCl electrode, with a Pt wire counter electrode), it is anticipated no other competing reactions will take place, and thus the fiber may be assumed to behave as an ideal capacitor; this can be verified by inspection of the resulting voltammagram. To find the capacitance, one uses the simple relationship C=dQ/dt/dV/dt. Where the sweep rate is experimentally set and the current is measured over time. Since the capacitance will also depend on the surface area of the fiber, by measuring out a specific length of fiber and measuring the specific surface area (either by using a nominal fiber diameter or through a means such as the Brunauer–Emmett–Teller method (BET) to measure the actual accessible surface area) one can calculate the specific capacitance of a fiber.

The specific capacitance of the fiber correlates quite strongly to how well the fiber has been oxidized, giving a simple measure of how intensely a fiber is oxidized in a specific treatment. In Figure 24, an intermediate-modulus fiber was subjected to a set of different oxidative treatments of various intensities. The capacitance of the fiber rose with the intensity of the oxidative treatment. At the same time, measures dependent on interfacial strength (such as open-hole tensile strength) can also be correlated with the fiber capacitance (Figure 24). Such a correlation suggests the use of capacitance as an indicator of interfacial strength. It also suggests that the mechanism of this change in strength may be related to, or at least covariant with changes in the specific capacitance, supporting the idea that interfacial oxygen content may play a role in interfacial bonding.

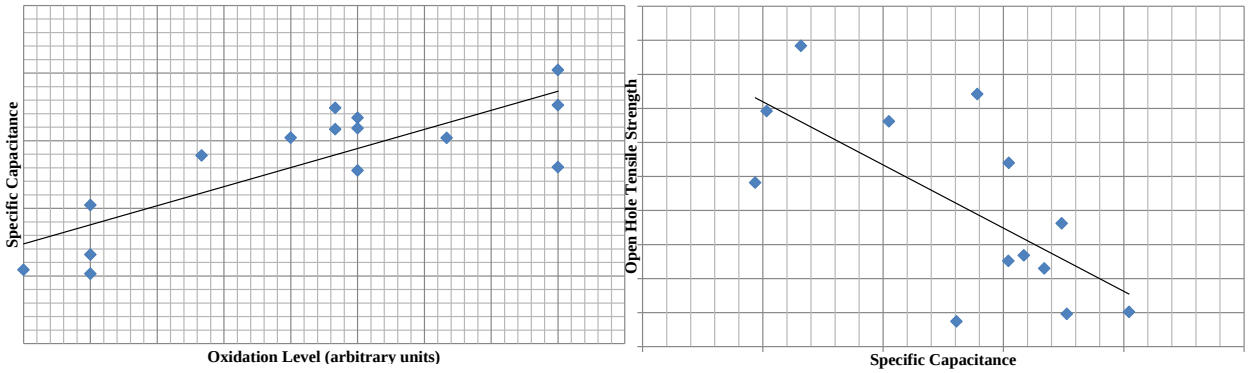

Figure 24: Left - Specific Capacitance versus degree of oxidation of an IM fiber, Right: Capacitance versus open-hole tensile strength

3.3.3 Porosimetery

Another method one can use to measure differences related to surface treatment is BET surface area via nitrogen adsorption. As mentioned above, this method can be used in conjunction with the specific capacitance. While there are reports in the literature that no significant difference in BET surface area has been observed for surface treated carbon fiber compared to non-surface treated carbon fiber, we have been using a method with a large sample size to measure this difference. (***13***) The surface area along with the pore size and volume present is a topic of interest as an increase in surface area will promote better bonding in a composite system and it has been reported that any microporosity present on the surface of carbon fibers likely plays a role in the chemical modification of the surface of carbon fiber. (***14***)

As we look at the surface of carbon fiber with nitrogen adsorption it is clear that the surface must be relatively smooth with few pores in the micro and meso porous range. The BET surface areas we typically measure on a range of CF products are approximately 0.5 m^2/g of fiber and the pore volumes are often south of 0.001 g/cc. In order to house enough sample to get accurate pore size and volume data we have been using a large sample cell which holds ~ 22-23 g of sample which gives us the required 10 m^2 of surface area for good data fidelity. A benefit of this is that we get very reproducible BET data (SD = 0.009 m^2/g).

Below in Figure 25 we are showing an example of nitrogen isotherms and pore size distributions for an IM carbon fiber before and after surface treatment. The measured multipoint BET surface area for the sample increases from 0.474 m^2/g to 0.587 m^2/g when surface treatment at this particular level is applied. The nitrogen isotherm clearly shows an increased uptake as a result of

the surface treatment. Some have suggested that the increase in surface area could be simply due to the removal of the so called "weak layer" which could expose additional surface area in the form of porosity. Another explanation is that some porosity is created as a result of the surface treatment process itself. If we could relate this increase in surface area somehow to chemical surface data we may be able to say that pores are important sites for the oxidation reactions which modify the surface

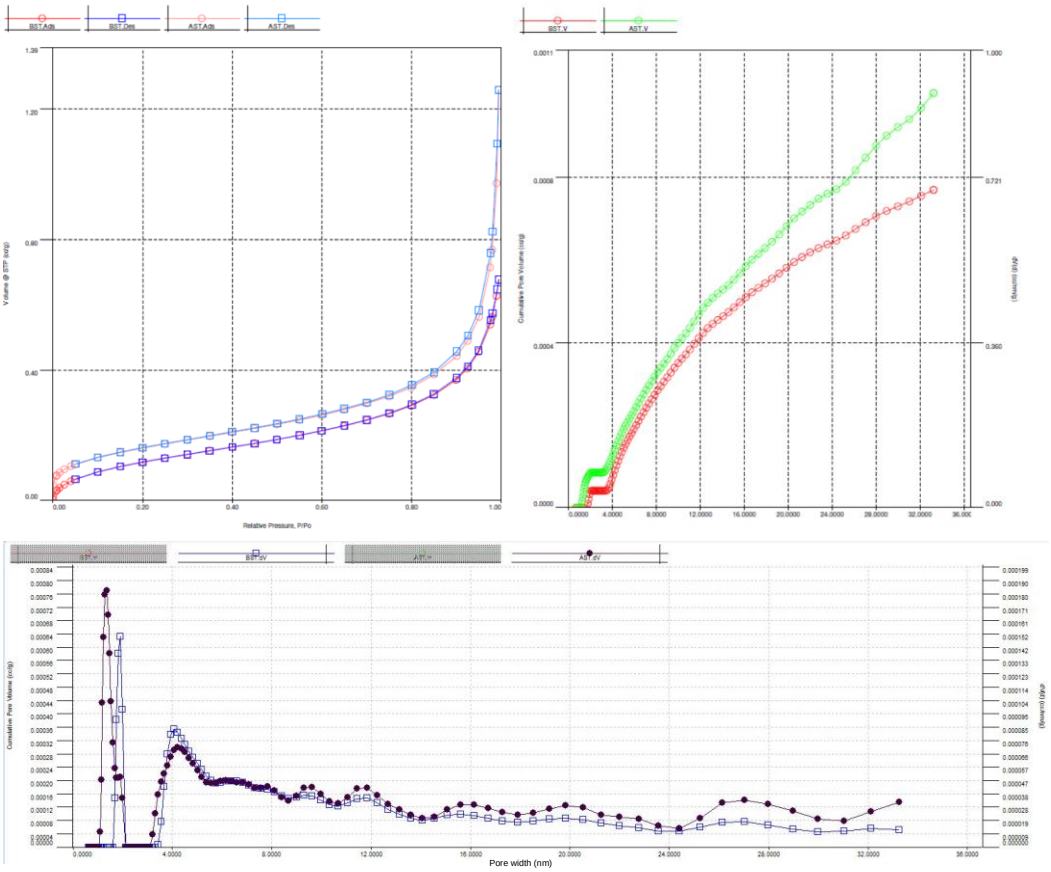

Figure 25: Top left-Nitrogen Isotherms, Top right- Cumulative pore volume, Bottom-Pore size distribution for IM CF before and after surface treatment

There is an increase in pore volume after surface treatment of the IM fiber. The cumulative pore volume is shown on the right side of Figure 25. The green line represents the fiber after surface treatment and it is clear there is an increase in pore volume for pores in the 12 nm and especially 28nm range. The total pore volume as measured at the end of the isotherm increases by over 85% as a result of the surface treatment. One can also see there is a slight shift in the smallest pore size measured before and after surface treatment from 1.9nm to 1.3nm. The cumulative pore volume does show an increase in actual pore volume in this region also. I am not sure why there would be more slightly smaller pores after surface treatment but this has been repeated for other samples.

4. CONCLUSIONS

A range of analytical techniques are required to track the structural changes in carbon fiber as it traverses the carbon fiber process. We have demonstrated the use of spectroscopy,

chromatography, porosimetery and SEM to observe these changes. We have also demonstrated how one can adjust process parameters to effect a change in the case where these analytical results are understood. It is evident that changes made to the carbon fiber process can affect composite properties independent of changes to the matrix. In any carbon fiber process it is critical that the manufacturer fully understand the structure and properties of the material leaving each unit operation and therefore it is critical to explore and understand analytical techniques that can provide this structural information.

5. REFERENCES

1. Shindo, Akio. "Studies on Graphite Fiber". The Industrial Research Institute: Osaka, 1961.
2. Johnson, J., Phillips, L.,Watt, W., British Patent 1,110,791, April 1965.
3. Shindo, Akio. Japanese Patent 28287, 1959.
4. Morgan, Peter. *Carbon Fibers and their Composites;* CRC Press: Boca Raton, Florida, 2005.
5. Mukhopadhyay, P., Schreiber, H. P. "Aspects of Acid-base interactions and use of inverse gas chromatography." *Colloids and Surfaces A: Physicochemical and Engineering Aspects* 100 (1995**):** 47-71.
6. Perret, R., Ruland, W. "The microstructure of PAN-based carbon fibers." *Journal of Applied Crystallography 3* (6) (1970): 525-532.
7. Donnet, J.B., Wang, T.K., Peng, J. C. M., Rebouillat, S., *Carbon Fibers*. New York: Marcel Dekker, 1998.
8. Thielmann, F., "Introduction into the characterization of porous materials by inverse gas chromatography." *Journal of Chromatography A* 1037(1-2) (2004): 115-123.
9. Huson, M., Church, J., Kafi, A., Woodhead, A. L., Khoo, J., Kiran, M. S. R. N., Bradby, J., Fox, B., "Heterogeneity of Carbon Fibre." *Carbon* 68 (2014)**:** 240-249.
10. Tang, L., Kardos, J. "A review of methods for improving the interfacial adhesion between carbon fiber and polymer matrix." *Polymer Composites 18* (1) (1997): 100-113.
11. Bleda-Martinez, M. J., Macia-Agullo, J. A., Lozano-Catello, D., Morallon, E., Cazorla-Amoros, D., Linares-Solano, A. "Role of surface chemistry on electric double layer capacitance of carbon materials." *Carbon 43* (13) (2005): 2677-2684.
12. Tabti, Z., Berenguer, R., Ruiz-Rosas, R., Quijada, C., Marallon, E., Cazorla-Amoros, D. "Electrooxidation Methods to Produce Pseudocapacitance-containing Porous Carbons." *Electrochemistry* 81(10) (2013**):** 833-839.
13. Harvey, J. "The characterization of carbon fiber surfaces by dye adsorption." *RAE Tech Memo Mat* (1975) *231*.
14. Tripathi, D., Kettle, A., Lopattananon, N., Beck, A., Jones, F. R. "Interface Molecular Engineering of Carbon Fiber Composites." *Proceedings of ICCM-11*.Gold Coast, Queensland, Australia, July 14-18, 1997**.** Australian Composites Structure Society. pp. 691-700.